Hindawi
Shock and Vibration
Volume 2023, Article ID 3082704, 10 pages
https://doi.org/10.1155/2023/3082704

Research Article

Dynamics of the Missile Launch from the Very Short-Range Mobile Firing Unit

Algimantas Fedaravičius, Karolis Jasas, Rimvydas Gaidys, and Kęstutis Pilkauskas

Kaunas University of Technology, Studentų St. 56, 51424 Kaunas, Lithuania

Correspondence should be addressed to Karolis Jasas; karolis.jasas@ktu.edu

Received 3 November 2022; Revised 10 March 2023; Accepted 14 March 2023; Published 1 April 2023

Academic Editor: Traian Mazilu

In this article, the results of research of dynamical processes during the first stage of a missile launch from very short-range mobile firing unit (MFU) are presented. The determined laws of motion of the system's components enabled determining characteristic motions that need to be reconstructed by the launcher simulator intended to be developed for personnel training. The half-car approach is applied for modelling the unit which consists of a vehicle and is attached to its missile launcher. The combined system is represented by a lumped-parameter model. The mathematical model is derived by applying the principle of Lagrange differential equations. Motion laws of the components of the system as its response to excitation load generated during missile launch were determined.

1. Introduction

In modern warfare, short-rangesurface-based air defence (SBAD) units play an important role in ensuring defence of troops from low flying aircraft such as helicopters and fighters. The typical layout of the very short-range mobile firing unit which has already proved its efficiency in practise is the short-range air defence system mounted on an armoured vehicle. Such a layout guarantees high mobility–fast entering of the unit to firing area, fast directing of the missiles to the launching position, their launching, and finally leaving the firing area by the unit. However, together, the very short-range mobile firing unit of this structure becomes a complex dynamical system. The characteristics of dynamical interaction of air defence system and the vehicle during the missile launching phase have an impact on dispersion of initial phase motion parameters of the missile and sequentially of target hitting. Here, two essential needs of deep understanding of dynamical performance of the unit can be outlined. First is to ensure the desired target covering characteristics by selecting parameters of the dynamical system. The second is to determine training procedures of personnel and to train in the most efficient way the personnel to operate the unit. For this purpose, a training simulator is intended to be developed which would reconstruct motions of the real short-range mobile firing unit, thus creating realistic perception of its dynamics by the operator during the simulated missile launch.

The importance of the research of the interaction of rocket/missile launcher has been understood as the era of intensive development of rocket artillery and other surface-based missile units started. E.g., the authors of [1] are a fundamental reference source intended to be used by rocket/missile systems developers. In it, the behaviour of the rocket and its launcher is presented as interaction of solid bodies under the effect of gravity, reaction forces, and rocket thrust forces what enables selection of the system's parameters ensuring the most effective launching process. Lee and Wilms [2] use the concept of a launcher as a solid body supported by torsional elastic and damping elements. The mathematical model for the analysis of the launcher motions when an interaction with the rocket and its free motion after leaving the rocket is derived. The effect of the blast force generated by the exhaust gas on the launcher is evaluated.

The principle of rigid bodies interacting through elastic and damping elements is applied by Cochran [3]. The proposed three degree-of-freedom model is applied for rocket launcher and launcher ground surface interaction analysis, and the impact of the parameters resulting in mal launch of the rocket was established.

The research of surface-based firing units with the focus on determining their dynamical properties and achieving their best effectiveness has been carried out by Dziopa and Nyckowski. In [4], the results of experimental tests of the ZMSU weapon module during the launch of unguided missiles are presented revealing that the characteristics of tilt motion of the launcher are presented. Using lumped parameter approach, the module is modelled as the system composed of mass, elastic, and damping elements. By the simulation results, which are in agreement with the experimental ones, it was shown that the parameters of both the launcher and the vehicle have an impact on dynamics of tilt motion of the launcher. In [5], the vibration control of the results of research carried out on the launcher turret vibration control during the rocket launch phase using lumped parameter model is presented. The proposed hybrid vibroisolation system allows stabilizing the turret motion by reducing disturbances occurring due to vibrations excited by road and missile firing inputs. Krzysztofik and Koruba [6] researched the problem of increasing precision of the guiding system of antiaircraft missile launcher mounted on a moving carrier vehicle when vibrations of the launcher due to excitations on the vehicle from the road are generated. For the system modelled by lumped parameter approach, adaptive control system is proposed.

The similar approach of the mass, elastic, and damping element system is applied for the analysis of the dynamical behaviour of the machine gun—vehicle interaction [7]. With the use of the same principle, dynamics of stand-alone (no vehicle) short-range air defence system is researched [8].

A number of research publications concerning the system of analogous structure MLRS (multiple launch rocket system) are available as well. In reference [9], MLRS is presented as a multibody system consisting of rigid bodies representing the vehicle and the launcher and elastic bodies in the form of elastic beams representing launching tubes. All bodies are interacting through elastic damping elements. With the aim of reducing ammunition consumption during the standard firing precision test, launch dynamics model, eigenfrequency equations, and dynamics response equations are established, dynamics response is simulated, the results are verified by a series of tests directly, and, finally, firing test scheme allowing significant reduction of rocket consumption is proposed.

In reference [10], the problem of improving the dispersion characteristics of the rockets is analysed. The dynamic model of motor-mechanism coupling system used for positioning the rocket at the necessary elevation and azimuth angles is derived using the Lagrange method, and the strategy of neural network predictor-based control system is proposed.

In reference [11], the efficient modelling method of MLRS as a coupled rigid-flexible multibody system is discussed. In the article, the focus is made on launching subsystem as the multibody system comprising the rocket, flexible tube, and tube tail. The rocket and tube tail are represented as rigid bodies and the flexible tube as a Euler–Bernoulli beam. Integrating the developed model of the launch subsystem with the vehicle model through elastic joints, dynamic response of the tube tip and the rocket is obtained.

In reference [12], the results of dynamic analysis of rocket launcher intended to fire rockets of different weights and geometric configurations moving on launch rail are presented. The system is made up of solid bodies representing the launcher and the vehicle and the deformable one representing the launch rail. The derived equations of motion enable analysis of oscillatory motion of the rocket launching system.

Summarising it can be stated that the systems missile/rocket launcher–vehicle are researched rather well aiming to determine the parameters of launch dynamics. Nevertheless, results of research conducted to reconstruct motion dynamics by a mobile firing unit simulator are not available.

Generally, training consists of class lectures, class simulators, and firing at targets with actual missiles. But the missiles are expensive, and usually, it is necessary to make a number of launches to be adequately prepared. Therefore, to have field training, equipment to replace actual shootings is important for efficiency in the training process.

Thus, with the aim of developing equipment that ensures efficient training of mobile missile unit personnel, research on characteristic behaviour of the unit that should be reconstructed by a simulator should be carried out.

2. Dynamical Model of the Missile Launch from the Very Short-Range MFU

In order to determine characteristic motion laws of the dynamical system missile launcher–vehicle, "half-car model" was selected; i.e., planar motion of the system is analysed [13, 14]. The results of the literature review presented in the previous section show that this approach allows obtaining the results with sufficient accuracy, which is approved by the results of experimental testing [15]. The body of the truck (vehicle) and short-range air defence system are represented by lumped masses interacting through massless elastic and damping elements. Vehicle suspension is modelled as a mass spring damper system. The developed model is presented in Figure 1. It represents the first stage of the missile launch motion, the period when under the effect of starting engine, the missile is thrown out of the launching tube. The model is a five DOF model with five depended variables (q_1, q_2, q_3, φ_1, φ_2). The system includes five inertia elements: m_1, m_2, m_3, m_4, I_3 where m_1-unsprung mass of the truck's suspension representing the front axle and associated with it parts; m_2-unsprung mass of the truck's suspension representing the rear axle and associated with it parts; m_3-sprung mass representing body of the truck; m_4-mass of the launcher; I_3-mass moment of inertia of the truck body; q_1-coordinate of unsprung mass m_1 of the front suspension in vertical direction; q_2-coordinate of unsprung mass m_2 of the

rear suspension in vertical direction; q_3-coordinate of the sprung mass m_3 in vertical direction; φ_1-angular coordinate of the sprung mass m_3; φ_2-angular coordinate of the launcher; a_1-distance from the front suspension to the mass center of the truck's body; a_2-distance from the rear suspension to the mass center of the truck's body; a_3-distance between the mass center of the truck body and vertical suspension stand of the launcher; a_4-distance between the mass center of the truck and revolute joint attachment of the launcher; a_5-distance between the vertical suspension stand of the launcher and the revolute joint of its attachment; a_6-length of the launcher; a_7-distance between the center of mass center of the launcher and the revolute joint of its attachment; b_1-height from mass center of the launcher to the point of attachment of its horizontal suspension elements. The model includes elastic elements k_1, k_2, k_3, k_4, k_5, k_6 and viscous damping elements c_1, c_2, c_3, c_4, c_5, c_6 where k_1-stiffness of front tire of the truck, c_1-damping coefficient of front tire of the truck, k_2-stiffness of the elastic element of the front suspension, c_2-damping coefficient of the front suspension, k_3-stiffness of rear tire of the truck, c_3-damping coefficient of rear tire of the truck, k_4-stiffness of the elastic element of the rear suspension, c_4-damping coefficient of the rear suspension, k_5-stiffness in horizontal direction of the launcher's mounting components, c_5-damping coefficient in horizontal direction of the launcher's mounting components, k_6-stiffness in vertical direction of the launcher's mounting components, and c_6-damping coefficient in vertical direction of the launcher's mounting components. The angle of attack of the launcher is α_0. Excitation force generated during the first phase of the missile launch is $F(t)$.

3. Mathematical Model

For the derivation of the mathematical model for the system presented previously, the second-order Lagrange differential equations were applied:

$$\frac{d}{dt}\left(\frac{\delta E_k}{\delta \dot{q}}\right) - \frac{\delta E_k}{\delta q} + \frac{\delta E_p}{\delta q} + \frac{\delta D_{isp}}{\delta \dot{q}} = F, \tag{1}$$

where E_k-kinetic energy, E_p-potential energy, D_{isp}-damping energy, F-generalized force vector, q-generalized coordinates, and $\dot{q}$-generalized velocities.

Based on the constructed dynamical model (Figure 1) of the short-range air defence system, the expressions of the energies can be written as follows:

Kinetic energy:

$$E_k = \frac{1}{2} m_1 \dot{q}_1^2 + \frac{1}{2} m_2 \dot{q}_2^2 + \frac{1}{2} m_3 \dot{q}_3^2 + \frac{1}{2} m_4 \left(\dot{q}_3^2 + \dot{\varphi}_2^2 a_7^2\right) + \frac{1}{2} I_3 \dot{\varphi}_1^2. \tag{2}$$

Potential energy:

$$E_p = \frac{1}{2} k_1 q_1^2 + \frac{1}{2} k_3 q_2^2 + \frac{1}{2} k_2 [q_1 - (q_3 - a_1\varphi_1)] + \frac{1}{2} k_4 [q_2 - (q_3 + a_2\varphi_1)] + \frac{1}{2} k_5 [b_1\varphi_1 - (\varphi_2 a_5 \sin\alpha_0)]^2 + \frac{1}{2} k_6 [(\varphi_2 a_5 \cos\alpha_0) - (a_3\varphi_1 + q_3)]^2. \tag{3}$$

Damping energy:

$$D_{isp} = \frac{1}{2} c_1 \dot{q}_1^2 + \frac{1}{2} c_3 \dot{q}_2^2 + \frac{1}{2} c_2 [\dot{q}_1 - (\dot{q}_3 + a_1\dot{\varphi}_1)]^2 + \frac{1}{2} c_4 [\dot{q}_2 - (\dot{q}_3 - a_1\dot{\varphi}_1)]^2 + \frac{1}{2} c_5 [b_1\dot{\varphi}_1 - (\dot{\varphi}_2 a_5 \sin\alpha_0)]^2 + \frac{1}{2} c_6 [(a_1\dot{\varphi}_2 \cos\alpha_0) - (a_3\dot{\varphi}_1 + \dot{q}_3)]^2. \tag{4}$$

Then, after making the necessary rearrangements, the mathematical model of the system can be expressed by 5 second-order differential equations as follows:

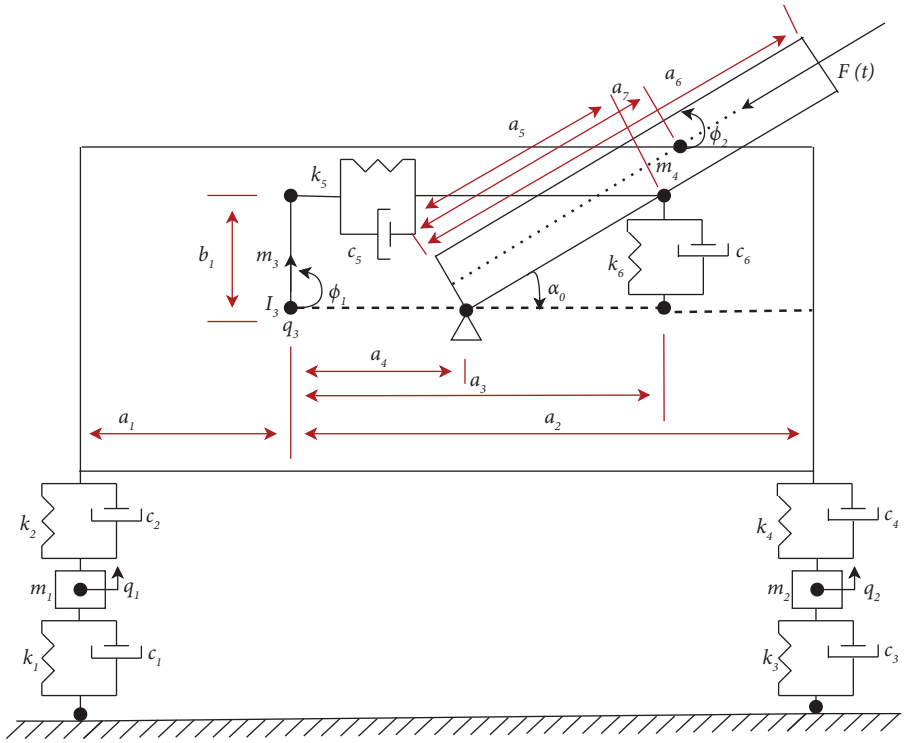

Figure 1: Dynamic model of the very short-range MFU.

$$
\begin{cases}
m_1\ddot{q}_1 + k_1q_1 + k_2[q_1 - (q_3 - a_1\varphi_1)] + c_1\dot{q}_1 + c_2[\dot{q}_1 - (\dot{q}_3 + a_1\dot{\varphi}_1)] = 0 \\
m_2\ddot{q}_2 + k_3q_2 + k_4[q_2 - (q_3 + a_2\varphi_1)] + c_3\dot{q}_2 + c_4[\dot{q}_2 - (\dot{q}_3 - a_1\dot{\varphi}_1)] = 0 \\
(m_3 + m_3)\ddot{q}_3 + k_2[q_1 - (q_3 - a_1\varphi_1)] + k_4[q_2 - (q_3 + a_2\varphi_1)] + \\
+k_6(a_5\varphi_2\cos\alpha_0 - a_3\varphi_1 - q_3) + c_2[\dot{q}_1 - \dot{q}_3 - a_1\dot{\varphi}_1] + \\
+c_4[\dot{q}_2 - \dot{q}_3 + a_1\dot{\varphi}_1] + c_6[a_5\dot{\varphi}_2\cos\alpha_0 - a_3\dot{\varphi}_1 - \dot{q}_3] = 0 \\
I_3\ddot{\varphi}_1 + k_2a_1(q_1 - q_3 + a_1\varphi_1) + k_4a_2(q_2 - q_3 + a_2\varphi_1) + k_5b_1(b_1\varphi_1 - \varphi_2a_5\sin\alpha_0) - \\
-k_6a_3(\varphi_2a_5\sin\alpha_0 - a_3\varphi_1 - q_3) + c_2a_1(\dot{q}_1 - \dot{q}_3 - a_1\dot{\varphi}_1) + c_4a_1(\dot{q}_2 - \dot{q}_3 + a_1\dot{\varphi}_1) + \\
+c_5b_1(b_1\dot{\varphi}_1 - \dot{\varphi}_2a_5\sin\alpha_0) - c_6a_3(a_5\dot{\varphi}_2\cos\alpha_0 - a_3\dot{\varphi}_1 - \dot{q}_3) = 0 \\
m_4\ddot{\varphi}_2a_7^2 - k_5a_5\sin\alpha_0(b_1\varphi_1 - \varphi_2a_5\sin\alpha_0) + k_6a_5\cos\alpha_0(a_5\varphi_2\cos\alpha_0 - a_3\varphi_1 - q_3) - \\
-c_5a_5\sin\alpha_0(b_1\dot{\varphi}_1 - \dot{\varphi}_2a_5\sin\alpha_0) + c_6a_5\cos\alpha_0(a_5\dot{\varphi}_2\cos\alpha_0 - a_3\dot{\varphi}_1 - \dot{q}_3) = F(t)
\end{cases}
\tag{5}
$$

With 5 generalized coordinates and 5 generalized velocities, this is a 10^{th} order model.

The excitation load that acts on the system is generated by the interaction of the missile and the launching tube during the first launch stage. The vehicle during launch is stationary, not moving. The missile–launch tube interaction is complex, including components due to the effect of gravity force with the moving application point, frictional interaction between the missile and the launching tube, jet effect of the exhaust gas on launcher's structure. Together, duration of this excitation load is very short. With the application of the research findings presented in articles [4–6], the excitation load was modelled as a force pulse of 0.05 s duration.

4. Numerical Simulation of the Dynamic Process

The simulation of dynamic processes using the derived mathematical model was performed using MATLAB software. The numerical values of the system parameters are given in Table 1.

The system of ordinary differential equations of second order is the mathematical model which was solved by the Runge–Kutta numerical method of the fourth order [18] with the application of the ODE45 Matlab function [19]. The response of the system as its reaction to the missile launch by the air defence system was obtained.

Table 1: Parameters of the system used for dynamical process modelling [7, 16, 17].

Parameters	Values
k_1 (kN/m)	647000
c_1 (kN s/m)	250
k_2 (kN/m)	500000
c_2 (kN s/m)	11000
k_3 (kN/m)	2400000
c_3 (kN s/m)	700
k_4 (kN/m)	1122000
c_4 (kN s/m)	54000
I_3 (kg m^3)	45591
k_5 (kN/m)	2000000
c_5 (kN s/m)	200000
k_6 (kN/m)	2000000
c_6 (kN s/m)	200000
a_1 (m)	2.94
a_2 (m)	2.68
a_3 (m)	1.3
a_4 (m)	1
α_0	30
a_5 (m)	0.6
a_6 (m)	1.64
a_7 (m)	0.82
b_1 (m)	0.43
m_1 (kg)	775
m_2 (kg)	1550
m_3 (kg)	3800
m_4 (kg)	80

While solving the ODEs, the initial conditions $q_1 = q_2 = q_3 = \varphi_1 = \varphi_2 = 0$ at the instant of time $t = 0$ s were used. The vehicle with antiaircraft weapon system is not moving. The excitation $F(t)$ is simulated as the force pulse of 0.05 s duration.

In Figures 2–4, displacements of the parts of the mobile antiaircraft weapon system after the launch are presented at different values of attack angle: $\alpha_0 = 30^\circ$, $\alpha_0 = 45^\circ$, $\alpha_0 = 60^\circ$ (see Figure 1). It can be observed that displacements of the truck's front suspension are the greatest at all angles of attack. The maximum value of the displacement of 0.017 m was obtained when the launcher attack angle is $\alpha_0 = 30^\circ$ (Figure 2). It was determined that after the launch, the front suspension moved up, while the rear suspension and the center of mass of the truck moved down. This could be explained by the fact that the launcher is attached not to the point of mass center of the truck but closer to the attachment point of the rear suspension of the truck. After 2 s, the transient dynamic process ends–the whole system truck–launcher transits to the steady state. For other values of the attack angle, the character of displacement evolution is the same just the maximum displacement values are lower. In all the cases, the duration of 2 s is necessary for transient process to decay.

Figure 5 shows angular displacements of the vehicle body and the launcher during the launch when the angle of attack $\alpha_0 = 30^\circ$. The angular coordinate of the launcher φ_2 during the launch immediately drops to 0.065 rad and in 2 seconds returns to the initial steady state position. The launch has the greatest impact on the generation of rotational vibrations of the launcher. The angular displacements of the truck body are not significant and fully decay in 2 s. According to the rotational displacements of the truck and launcher after the first launch, the second launch can be performed after 2 s.

Figure 6 presents the velocities of the inertia elements of the dynamic model during launch when the angle of attack $\alpha = 30^\circ$. The velocity dq_1 of the front suspension after the launch drops down till the 0.18 m/s and immediately increases till the 0.07 m/s. Maximum velocity dq_2 was obtained for rear suspension of the truck. Vibration modes of higher frequencies, which decayed after 1 s, were generated after the launch. Due to higher mass, stiffness, and damping coefficients, the lowest vibration velocities were obtained for the truck.

Figure 7 presents the angular velocities of the body of the truck and the launcher during the launch when the angle of attack $\alpha_0 = 30^\circ$ and the angular velocity of the launcher ($d\varphi_2$) after the launch drops down to 1.8 rad/s and immediately increases to 0.2 rad/s. The significantly higher angular velocity lasts for a short time interval of about 0.2 s and decays instantly. The angular velocity of the truck's body ($d\varphi_1$) due to the higher mass, stiffness, and damping coefficients is very low.

Accelerations of inertia elements of the dynamic model during launch when angle of attack $\alpha = 30^\circ$ are presented in Figure 8. Accelerations versus time graphs confirm the oscillatory decaying nature of the response to the excitation load generated by the launch process for all mass elements of the model. Maximum acceleration ($ddq_1 \approx -5.7$ m/s^2) was obtained for the unsprung mass of the front suspension of the truck. Acceleration of the body of the truck makes a few

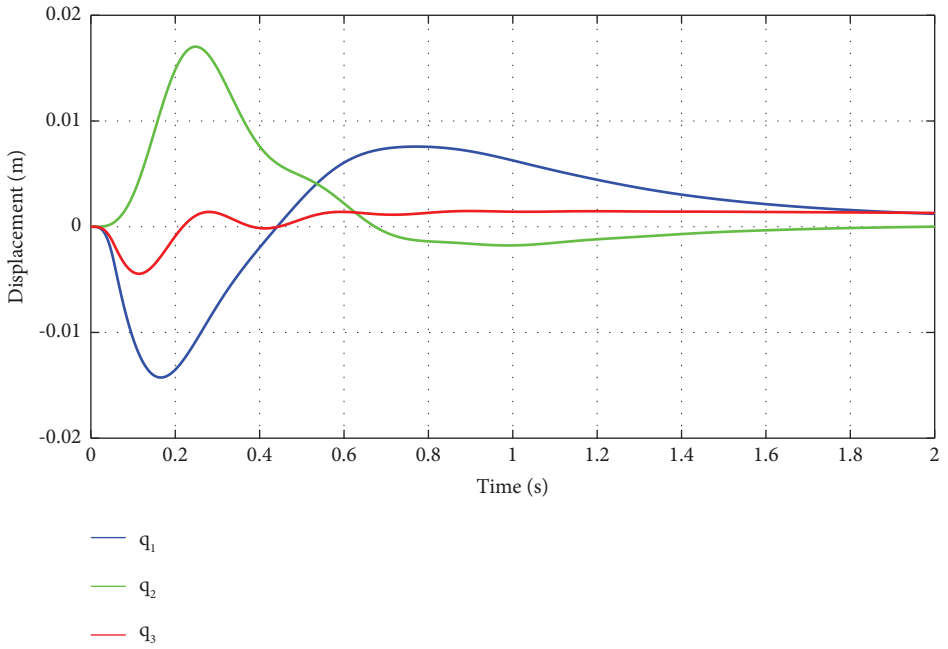

FIGURE 2: Displacements of parts of the mobile antiaircraft weapon system after launch at the angle of attack $\alpha_0 = 30^\circ$: q_1-vertical displacement of unsprung mass m_1 of the front suspension, q_2-vertical displacement of unsprung mass m_2 of the rear suspension, and q_3-vertical displacement of mass center of the vehicle body.

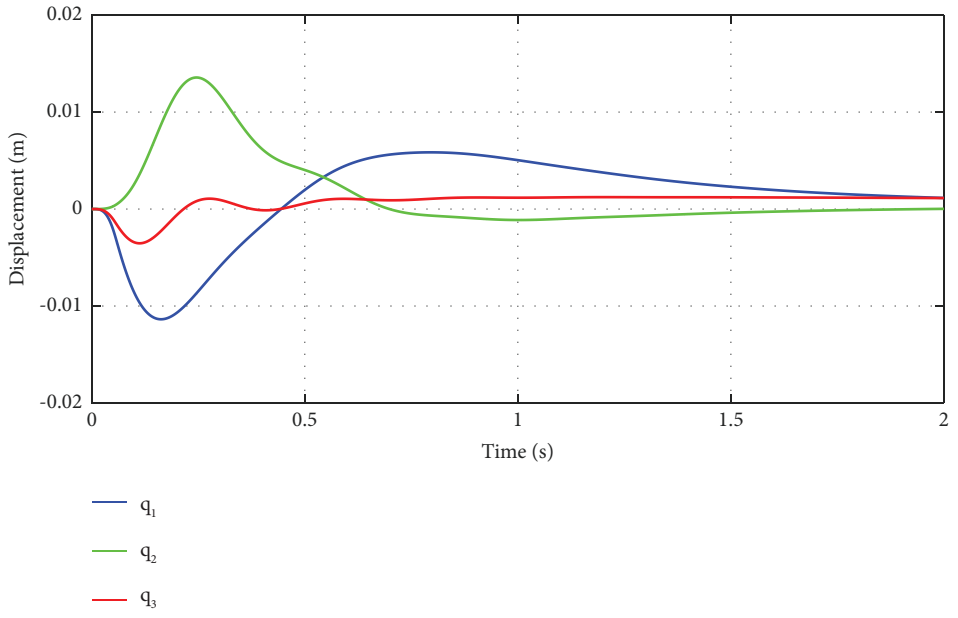

FIGURE 3: Displacements of parts of mobile antiaircraft weapon system after launch at the angle of attack $\alpha_0 = 45^\circ$: q_1-vertical displacement of unsprung mass m_1 of the front suspension, q_2-vertical displacement of unsprung mass m_2 of the rear suspension, and q_3-vertical displacement of mass center of the vehicle body.

cycles of decaying oscillations with a maximum amplitude of about 2 m/s^2.

Figure 9 presents the angular accelerations of the body of the truck and the launcher during launch when the angle of attack $\alpha_0 = 30^\circ$. The angular acceleration of the launcher ($ddfi_2$) shows an impulse type nature, sudden drop to −50 rad/s^2 and immediate increase to a value of approximately 270 rad/s^2 while the angular acceleration of the truck body is negligible compared to the acceleration of the launcher. The obtained accelerations versus time characteristics serve as primary information for the development of training simulator for the very short-range mobile firing

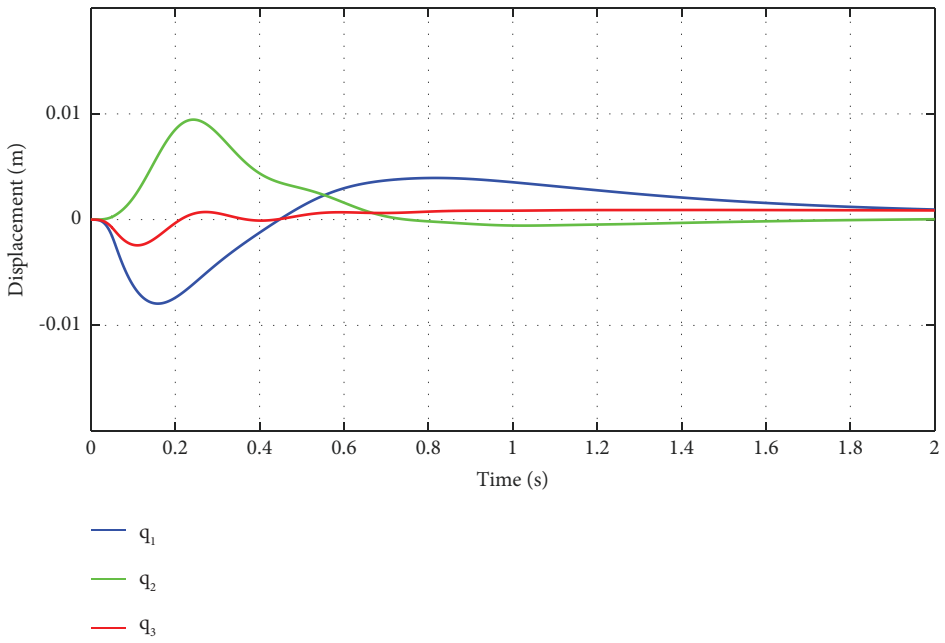

FIGURE 4: Displacements of parts of the mobile antiaircraft weapon system after launch at the angle of attack $\alpha_0 = 60^\circ$: q_1-vertical displacement of unsprung mass m_1 of the front suspension, q_2-vertical displacement of unsprung mass m_2 of the rear suspension, and q_3-vertical displacement of mass center of the vehicle's body.

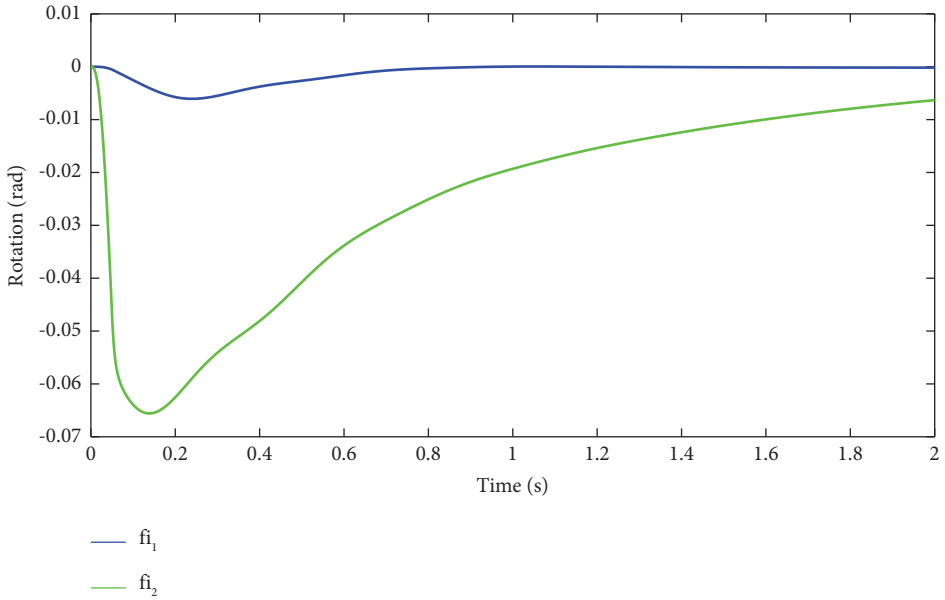

FIGURE 5: Angular displacements of parts of the mobile antiaircraft weapon system after the launch: φ_1-angular displacement of the vehicle's body and φ_2-angular displacement of the launcher.

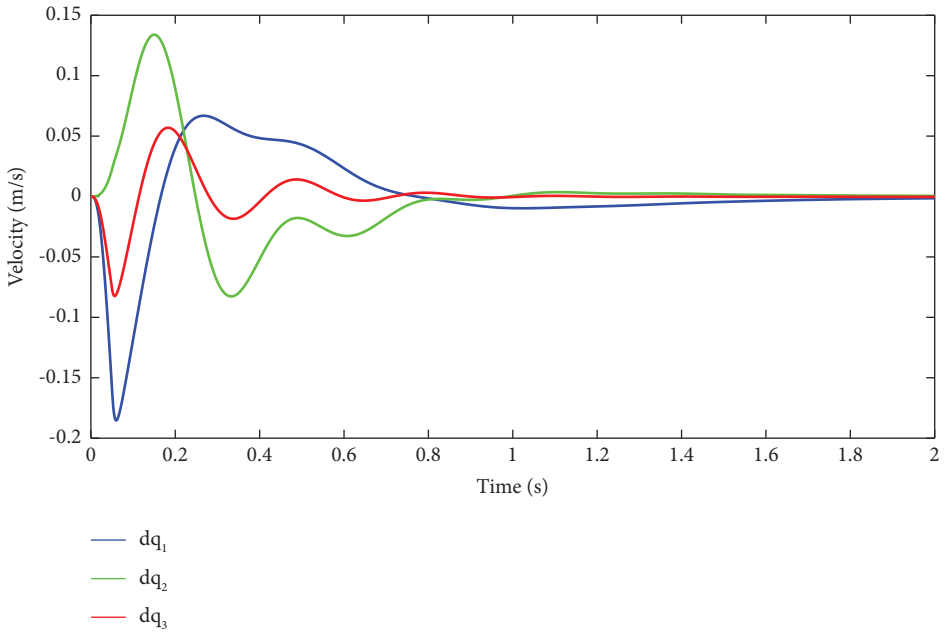

Figure 6: Velocities of the parts of mobile antiaircraft weapon system after the launch: dq_1-vertical velocity of front suspension of the truck, dq_2-vertical velocity of rear suspension of the truck, and dq_3-vertical velocity of the truck's mass center.

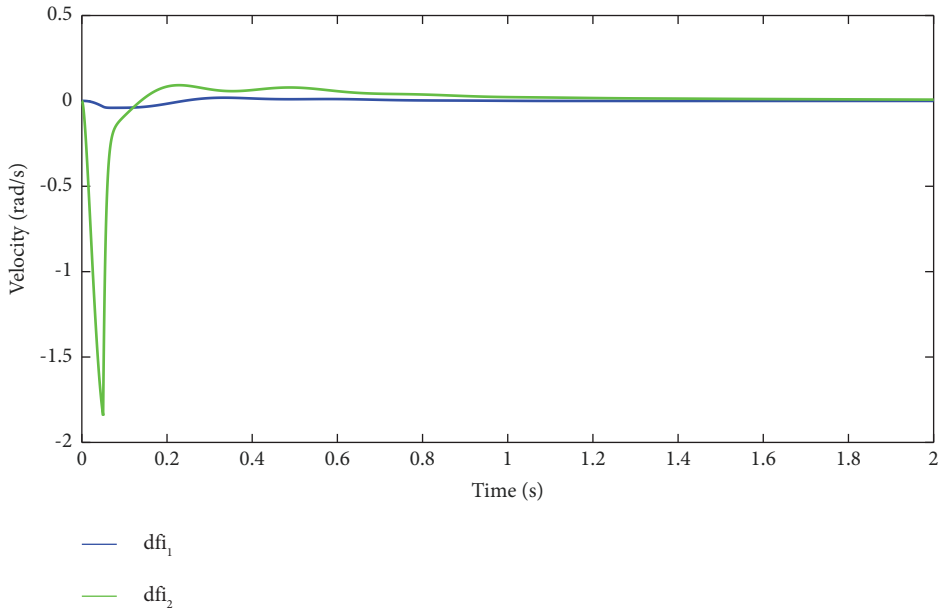

Figure 7: Angular velocities of parts of the mobile antiaircraft weapon system after the launch: $d\varphi_1$-angular velocity of the truck's body and $d\varphi_2$-angular velocity of the launcher.

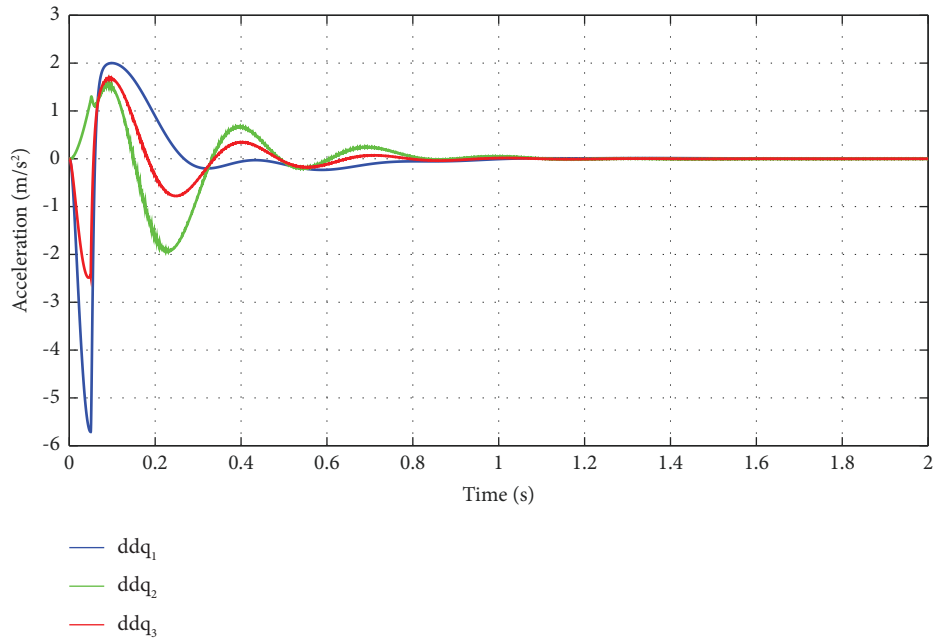

FIGURE 8: Accelerations of parts of the mobile antiaircraft weapon system after launch: ddq_1-vertical acceleration of front suspension of the truck, ddq_2-vertical acceleration of rear suspension of the truck, and ddq_3-vertical acceleration of the center of mass of the truck.

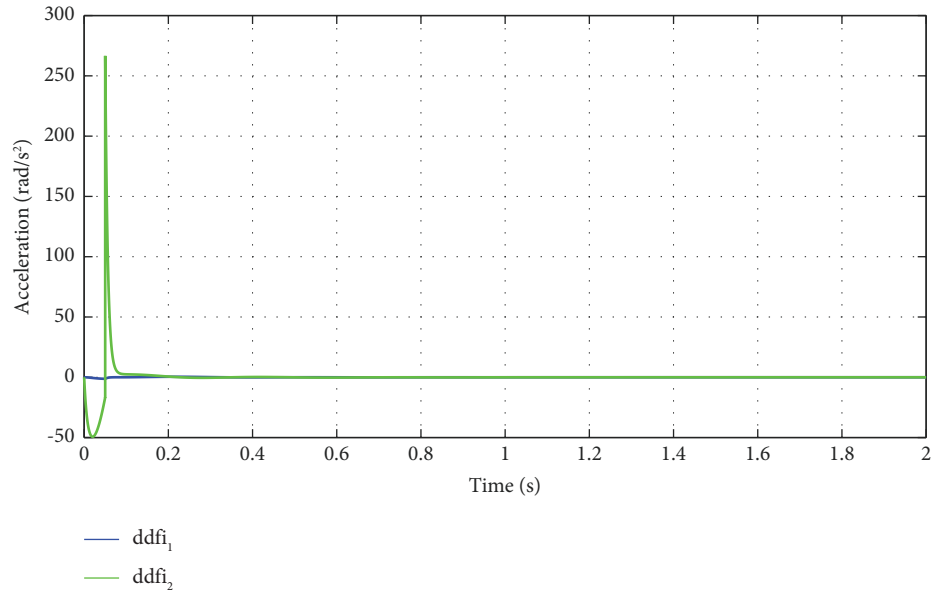

FIGURE 9: Angular accelerations of parts of the mobile antiaircraft weapon system after launch: $ddfi_1$-angular acceleration of the truck body and $ddfi_2$-angular acceleration of the launcher.

unit—the primary information allowing to determine excitation loads to be applied on the simulator's components representing truck's body and the launcher.

5. Conclusions

(1) A mathematical model of the short-range air defence system was derived in the form of the system of second-order ordinary differential equations (ODEs), which enables an efficient way to determine characteristic motions of the system during missile launch with the aim of being reconstructed by a launch simulator.

(2) The laws of motion in the linear and angular displacements of the truck body were obtained. Due to the excitation load generated by the missile launch, the highest displacements of 0.017 m appeared in the front suspension of the truck. Its unsprung mass moved up while the unsprung mass of the rear suspension moved down. Due to the fact that the

launcher is attached not to the point of mass center of the truck but closer to the attachment point of the rear suspension of the truck, angular motion of the body is observed.

(3) The launching load has the highest impact on the angular motion of the launcher. Due to the excitation load generated by the missile launch, angular coordinate of the launcher almost instantly dropped to the value of 0.065 rad and in 2 seconds returns to initial steady state position. Angular displacement of the body of the truck is not essential and therefore can be neglected.

(4) Peak velocity values of the unsprung masses of the truck suspension are observed in the time interval of 0.2 s. For the front suspension, these values are 0.18 m/s and 0.07 m/s, and for the rear suspension, 0.14 m/s and 0.8 m/s accordingly.

(5) The highest linear acceleration ($ddq_1 \approx -5.7\ \mathrm{m/s^2}$) was obtained for the unsprung mass of the front suspension of the truck, and the acceleration of the body of the truck shows the nature of decaying oscillations with a maximum amplitude of about $2\ \mathrm{m/s^2}$. Impulse-type nature of the angular acceleration of the launcher ($ddfi_2$) is observed, while the angular acceleration of the body of the truck is negligible compared to acceleration of the launcher.

(6) The laws of motion obtained and their kinematic parameters allow the principal assumption that, using the obtained quantitative and qualitative simulation data, the dominant angular motion of the launcher and the linear motions of the truck body need to be reconstructed by the training simulator for the very short-range mobile firing unit.

Abbreviations

MFU: Mobile firing unit
SBAD: Surface-based air defence
ODEs: Second-order system of ordinary differential equations.

Data Availability

The data used in this article are available from the corresponding author upon reasonable request.

Conflicts of Interest

The authors declare that there are no conflicts of interest regarding the publication of this paper.

References

[1] B. V. Orlov, *Design of Rocket and Barrel Systems*, Mashinostrojenije Moscow, Russia, 1974.

[2] S. K. Lee and E. V. Wilms, "Analysis of missile launchers, Part J, phase 1: FourDegree of freedom multiple launcher," University of Illinois, T&AM Report 188, 1961.

[3] E. J. Cochran, "Investigation of factors which contribute to mallaunch of free rockets," Technical Report RL-CR-76-4, Auburn University, Alabama, 1975.

[4] Z. J. Dziopa and M. Nyckowski, "Modelling and testing the dynamic properties of a launcher with unguided missiles," *Problems of Mechatronics Armament Aviation Safety Engineering*, vol. 13, no. 4, pp. 51–66, 2022.

[5] Z. Dziopa and Z. Koruba, "The impact of launcher turret vibrations control on the rocket launch," *Bulletin of the Polish Academy of Sciences, Technical Sciences*, vol. 63, no. 3, pp. 717–728, 2015.

[6] I. Krzysztofik and Z. Koruba, "Adaptive control of anti-aircraft missile launcher mounted on a mobile base," *Theoretical and Applied Mechanics Letters*, vol. 2, no. 4, Article ID 043008, 2012.

[7] A. Fedaravičius, V. Jonevičius, A. Survila, and A. Pincevičius, "Dynamics study of the carrier HMMWV M1151," *Journal of Vibroengineering, Vibromechanika, Lithuania Academy of Science*, vol. 15, no. 3, pp. 1619–1626, 2013.

[8] A. Fedaravičius, K. Jasas, E. Sližys, and A. Survila, "Modeling of the missile launch dynamic processes in short-range air defense system," *Mechanics*, vol. 28, no. 1, pp. 32–37, 2022.

[9] Y. Miao, G. Wang, X. Rui, and T. Tu, "Study on test dynamics method of non-full loading firing for multiple launch rocket system," *Mechanical Systems and Signal Processing*, vol. 122, pp. 463–479, 2019.

[10] B. Li, X. Rui, W. Tian, and G. Cui, "Neural-network-predictor-based control for an uncertain multiple launch rocket system with actuator delay," *Mechanical Systems and Signal Processing*, vol. 141, Article ID 106489, 2020.

[11] Q. B. Zhou, X. T. Rui, G. P. Wang, and J. S. Zhang, "An efficient and modular modeling for launch dynamics of tubed rockets on a moving launcher," *Defence Technology*, vol. 17, no. 6, pp. 2011–2026, 2021.

[12] D. Vujic, V. Djurkovic, and N. Milenkovic, "Slavisa trajkovic, dynamic analysis of rockets launcher," *Technical Gazette*, vol. 28, no. 2, pp. 530–539, 2021.

[13] K. Popp and W. Schihlen, *Ground Vehicles Dynamics*, Springer, Berlin, Germany, 2010.

[14] R. N. Jazar, *Vehicle Dynamics: Theory and Application*, Springer, Berlin, Germany, 2008.

[15] P. Droppa and M. Stiavnicky, "Vibrations simulation of wheeld vehicles," *Problems of Mechatronics (Armament, Aviation, Safety Engineering)*, vol. 2, no. 8, 2012.

[16] R. X. Xia, J. H. Li, J. He, and D. F. Shi, "Effect analysis of vehicle system parameters on dynamic response of pavement," *Mathematical Problems in Engineering*, vol. 2015, Article ID 561478, 8 pages, 2015.

[17] M. A. Abdelkareem, M. M. Makrahy, A. M. Abd-El-Tawwab, M. Moheyeldein, and M. M. Moheyeldein, "An analytical study of the performance indices of articulated truck semi-trailer during three different cases to improve the driver comfort," *Proceedings of the Institution of Mechanical Engineers - Part K: Journal of Multi-body Dynamics*, vol. 232, no. 1, pp. 84–102, 2018.

[18] Wolfram Math World, "Runge-kutta Method, Wolfram Math World," 2022, https://mathworld.wolfram.com/Runge-KuttaMethod.html.

[19] O. Simon, O. M. A. A. Olusegun, O. Olatokunbo, and O. Olatokunbo, "Integration of finite element method with Runge – kuta solution algorithm," *International Journal of Engineering Research in Africa*, vol. 7, no. 4, pp. 45–50, 2017.